Journal of Power Sources 187 (2009) 500–504

Contents lists available at ScienceDirect

Journal of Power Sources

journal homepage: www.elsevier.com/locate/jpowsour

Short communication

Plasma nitrided titanium as a bipolar plate for proton exchange membrane fuel cell

Jing Liu, Fei Chen, Yongguo Chen, Dongming Zhang*

State Key Laboratory of Advanced Technology for Materials Synthesis and Processing, Wuhan University of Technology, Wuhan 430070, PR China

ARTICLE INFO

Article history:
Received 8 November 2008
Accepted 12 November 2008
Available online 28 November 2008

Keywords:
Plasma nitriding
Titanium bipolar plates
XRD
SEM
Interfacial contact resistance
Polarization curve

ABSTRACT

Plasma nitriding was applied to improve the surface performance of titanium bipolar plate. XRD and SEM results showed a titanium nitride layer was formed after nitridation. In comparison with pure titanium, the interfacial contact resistance of plasma nitrided titanium was reduced to some extent by the nitridation treatment. However, high corrosion current was observed under electrochemical tests in 0.5 M H_2SO_4 + 5 ppm HF. Both the electrical conductivity and corrosion resistance of the surface of plasma nitriding titanium did not reach the level of graphite. Some more improvements are expected in the plasma nitriding process or another surface modification on pure titanium.

1. Introduction

Proton exchange membrane (PEM) fuel cell [1–3] is one of the most promising power generation sources for mobile and stationary applications because of its superior properties such as low temperature operation and rapid start-up. Bipolar plates [4–6], which can distribute the fuel and oxygen to the anode and cathode and provide the electrical contact between adjacent cells, are significantly used in PEM fuel cells.

Currently, bipolar plates are generally applied in terms of the graphitic materials [7–9]. However, the high processing cost of graphite bipolar plate inhibits its application in fuel cells. Compared to the graphite materials, the metallic materials have many advantages such as low-cost, good bulk electrical and thermal conductivities, excellent mechanical properties and machinability, which are effective to be used as bipolar plates. However, electrochemical corrosion may occur when the metallic bipolar plates are used in contact with acidic electrolyte, which can also lead to the dissolution of metallic ion. The metallic ions are diffused into the membrane, which is attributed to the poisoning of the membrane electrode assembly (MEA) and decrease of the output of fuel cells. Moreover, a relative high interfacial contact resistance can be caused by the passive film on the metal surface. Therefore, single metal or alloy is not suitable for bipolar plates application. It is reported in the previous studies [10–12] that surface modification can be applied to improve the surface performance of metals.

Plasma nitriding [13–16] is a promising chemical heat treatment process, which is widely used in industrial application. In this study, titanium was chosen as the substrate material. After nitridation, titanium nitride layer was formed by reaction between the titanium substrate and nitrogen. Titanium nitride films, which have good electrical conductivity and corrosion resistance, were widely used in industry. Compared with the pure titanium and graphite, plasma nitrided titanium showed some enhanced properties.

2. Experimental procedures

2.1. Test material and plasma nitriding procedure

Annealed grade industrial titanium sheets, purchased from Dingyu Titanium Inc. Baoji, Shaanxi Prov., China, were in the size of 25 mm × 25 mm × 4 mm and used as the substrate material. The surface of the as-purchased titanium was polished by using SiC polishing paper and alumina paste before the plasma nitriding process. Plasma nitriding was then carried out in a LDMC-AQK (produced by Wuhan Plasma Technol. Res. Inst., Wuhan, Hubei Prov., China) plasma facility. The plasma nitriding parameters are listed in Table 1.

2.2. Characterization

2.2.1. Phase compositions and microstructure

The pure titanium and plasma nitrided titanium were examined by X-ray diffraction (XRD) using a Philips X-ray diffractometer oper-

* Corresponding author. Tel.: +86 27 87217002 fax: +86 27 87879468.
E-mail address: zhangdongming71@whut.edu.cn (D. Zhang).

0378-7753/$ – see front matter © 2009 Published by Elsevier B.V.
doi:10.1016/j.jpowsour.2008.11.086

Table 1
LDMC-AQK plasma nitriding parameters.

Technical parameters	Value
Temperature (K)	1173
Pressure (Pa)	400
Time (h)	4
Gas composition	Pure N_2
Gas flow rate ($L\,min^{-1}$)	4–5
Voltage (V)	600–800
Current (A)	4–6

ated at $V = 40$ kV, $I = 40$ mA and Cu Kα radiation. The surface and profile of plasma nitrided titanium were observed by SEM using S3400-N. EDS was also used to detect the elements.

2.2.2. Interfacial contact resistance

Fig. 1 exhibits the simulated PEMFC arrangement for evaluation of interfacial contact resistance. The test sample was sandwiched between two pieces of carbon paper which was used to simulate the gas diffusion, as shown in Fig. 1(a). The test sample was thoroughly cleaned by ethanol, following by washing with distilled water and dried in air. For calculation, one carbon paper was sandwiched between two copper plates, as shown in Fig. 1(b). The copper plates in both two arrangements were polished before measurement. An electrical current (2 A) was passed through the two arrangements and by measuring the potential differences at different compaction forces, it was possible to calculate the interfacial contact resistance correlated to compaction force according to the following equation:

$$R_{tot} = \frac{VA_s}{I} \quad (1)$$

where R_{tot} is the total interfacial contact resistance, V is the potential, I is the current and A_s is the surface area of the test sample.

According to Fig. 1(a), the total resistance of $R_{tot}(a)$ consists of:

(1) the bulk resistances of two copper plates, $2Rcu$;
(2) two interfacial contact resistances between copper plate and carbon paper, $2Rc/cu$;
(3) the bulk resistances of two carbon paper, $2Rc$;
(4) two interfacial contact resistances between carbon paper and sample, $2R_{C/Ti}$;
(5) the bulk resistance of the sample, R_{Ti}, and the outside total resistance, R_0.

$$R_{tot}(a) = 2Rcu + 2R_{C/Cu} + 2Rc + 2R_{C/Ti} + R_{Ti} + R_0 \quad (2)$$

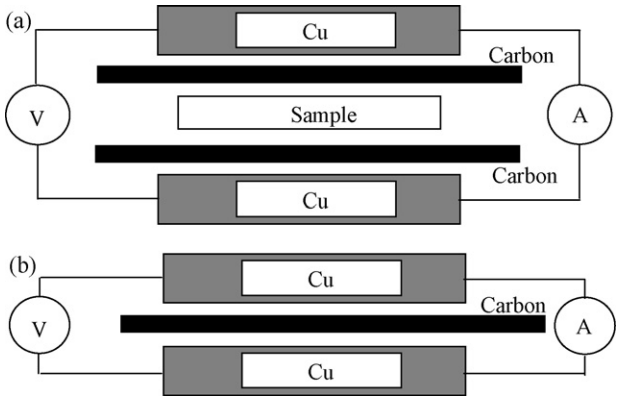

Fig. 1. Schematic illustration of the test for interfacial contact resistance. (a) The test sample is sandwiched between two pieces of carbon paper to test the total resistance, and (b) only carbon paper is sandwiched between the cupper plates for the calculation of the carbon paper and copper.

According to Fig. 1(b), the total resistance of $R_{tot}(b)$consists of:

(1) the bulk resistances of two copper plates, $2Rcu$;
(2) two interfacial contact resistances between copper plate and carbon paper, $2Rc/cu$;
(3) the bulk resistance of carbon paper, Rc, and the outside total resistance, R_0.

$$R_{tot}(b) = 2Rcu + 2R_{C/Cu} + Rc + R_0 \quad (3)$$

From Eqs. (2) and (3), the interfacial contact resistance $R_{C/Ti}$ between the sample and gas diffusion layer (carbon paper) can be calculated by using the following equation:

$$R_{C/Ti} = \frac{R_{tot}(a) - R_{tot}(b) - Rc - R_{Ti}}{2} \quad (4)$$

where Rc and R_{Ti} can be calculated according to their bulk resistivities, which can be measured by the four-point probe method [17]. The resistances of carbon paper, pure titanium and plasma nitrided titanium can be calculated by using the following equation:

$$R = \rho\frac{l}{A_s} \quad (5)$$

where R is the bulk resistance, ρ is the bulk resistivity, l is the thickness, A_s is the surface area.

2.2.3. Electrochemical

In order to analyze the corrosion resistance of pure titanium, plasma nitrided titanium and graphite, a conventional three-electrode system was used in the electrochemical test. The polarization curves of different samples were performed in a self-regulating electrobath in which a platinum sheet acted as the counter electrode, a mercury sulfate electrode (MSE, 0.650 V vs. NHE) was used as the reference electrode. In the potentiodynamic test, the initial potential was −1.5 V vs. MSE, and the final potential was 1.5 V vs. MSE, and the scanning rate was $10\,mV\,s^{-1}$. The electrolyte was 0.5 M H_2SO_4 + 5 ppm HF. The test was conducted from the start to the end at room temperature without any gas purging.

3. Results and discussion

3.1. Microstructure

After plasma nitriding, the surface of the pure titanium turned to a shiny golden color. XRD patterns of the surface of the pure titanium and plasma nitrided titanium are presented in Fig. 2. The

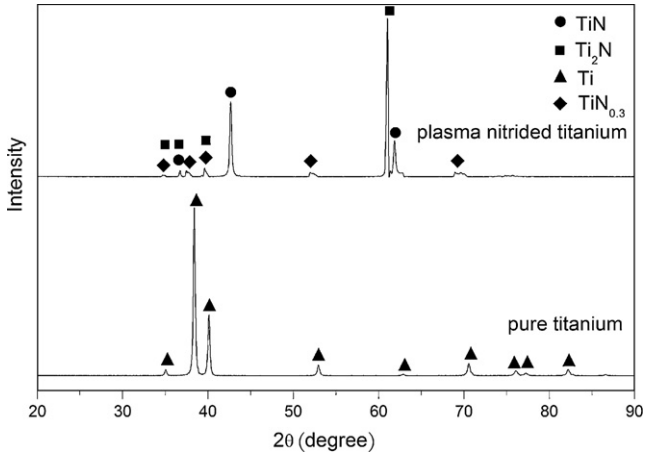

Fig. 2. X-ray diffraction (XRD) patterns of the pure titanium and plasma nitrided titanium.

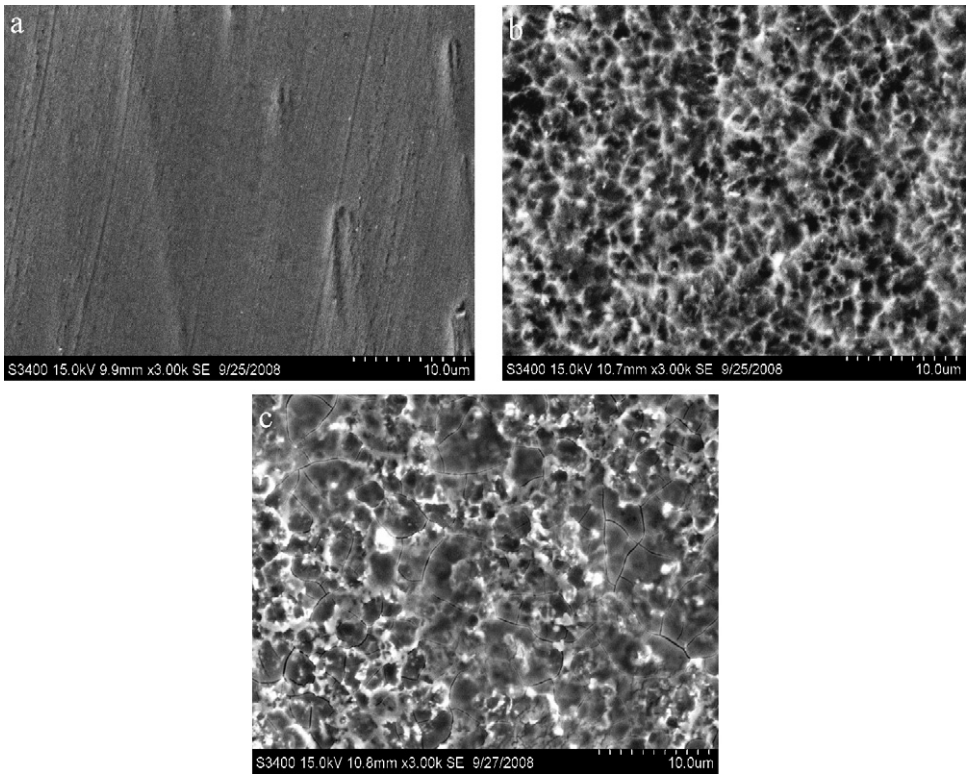

Fig. 3. SEM images of the surface of: (a) pure titanium, (b) plasma nitrided titanium, and (c) plasma nitrided titanium after electrochemical test.

presence of the TiN, Ti_2N and $TiN_{0.3}$ phases on the surface of the nitridated titanium indicate the formation of titanium nitride after plasma nitridation of pure Ti. No Ti phase is detected, indicating the formation is complete.

SEM images of the surface of the pure titanium and plasma nitrided titanium are shown in Fig. 3. It is observed clearly that the surface of pure titanium is very smooth and dense, shown in Fig. 3(a), while the surface is coarse after nitridation, shown in Fig. 3(b). The grain morphology and grain boundaries of the titanium nitride are clearly seen on the surface of the plasma nitrided titanium after electrochemical test, shown in Fig. 3(c).

Fig. 4 exhibits the SEM and EDS images of the cross-section profile of the plasma nitrided titanium. It is seen from the SEM image that a compound layer is clearly observed on the pure titanium substrate and its thickness is ~3 μm. The white line marked in Fig. 4(a) is the EDS results for the lining elements scan. A quantitative composition was measured on the plasma nitrided titanium by means of EDS. Fig. 4(b) displays the atomic concentrations of N and Ti, along the cross-section of the specimen. It is seen clearly that along the line scan direction, the nitrogen element content is decreased and titanium element content is increased from the film to the substrate. This fluctuation is apparently observed at 3 μm or less from the top surface while neither N nor Ti element content changes at 4 μm or greater, indicating that after nitridation, the titanium nitride compound is formed and a gradient structure is obtained.

3.2. Interfacial contact resistance

The interfacial contact resistances of different test samples are measured at different compaction forces, as shown in Fig. 5. It is observed that the contact resistance is decreased with increasing the compaction force, which is the same result to the published reference [18–20]. This is because the effective contact area is increased with increasing the pressure, namely the enhanced the electrical conductivity. However, when the pressure is increased to

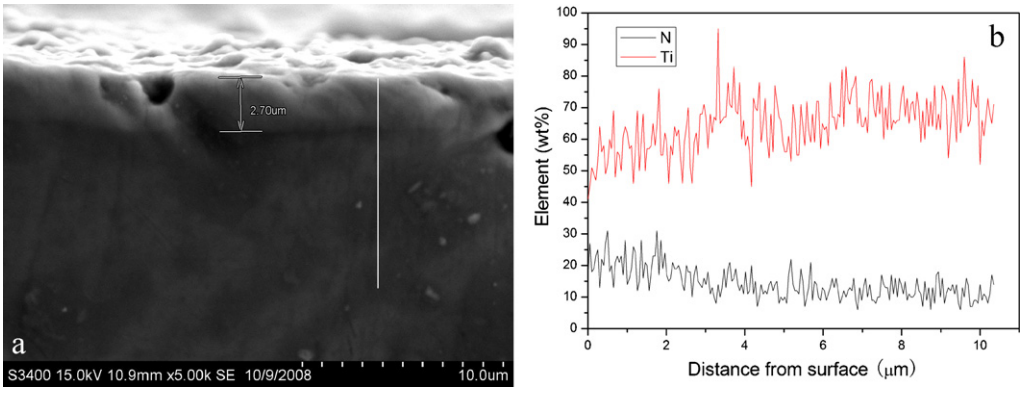

Fig. 4. SEM (a) and EDS (b) images of the cross-section profile of the plasma nitrided titanium.

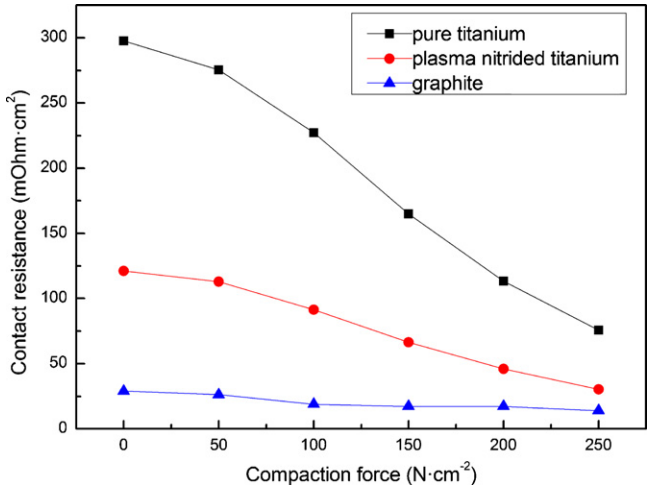

Fig. 5. Effect of compaction force on the contact resistance of different samples.

Table 2
Interfacial contact resistances of pure titanium, plasma nitrided titanium and graphite (220 N cm^{-2}).

	Interfacial contact resistance (mΩ cm^2)
Graphite	15.43
Plasma nitrided titanium	38.58
Pure titanium	96.91

a certain value, the effective contact area is not increased any more, and no apparent change is seen thereafter.

Table 2 exhibits the exact interfacial contact resistances for pure titanium, plasma nitrided titanium and graphite results at the compaction force of 220 N cm^{-2}. Compared with pure titanium, plasma nitrided titanium sample shows a smaller variation, indicating the influence of TiN coating is quite limited. Moreover, the interfacial contact resistance of plasma nitrided titanium is reduced when compared to the pure titanium sample. This is because after nitridation, the oxide film which has poor electrical conductivity on the pure titanium has been replaced by the nitrided film which has good electrical conductivity, as clearly seen in Fig. 4(a). It is also seen clearly that graphite shows the best interfacial contact resistance, so more improvements are needed in the surface modification of titanium bipolar plates.

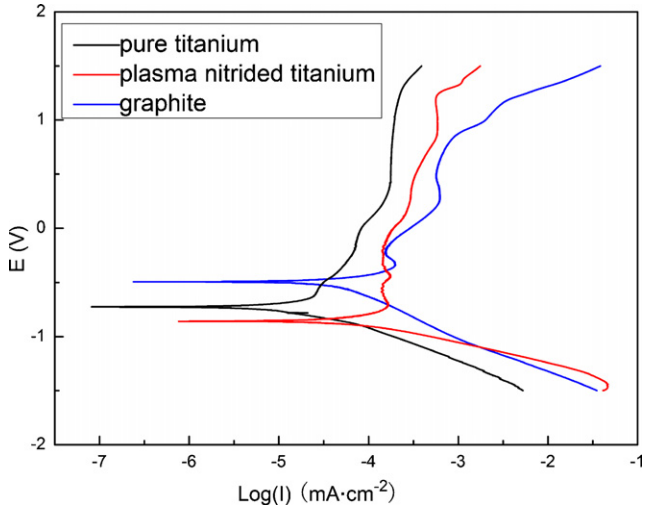

Fig. 6. Polarization curves of pure titanium, plasma nitrided titanium and graphite.

Table 3
Electrochemical test results in 0.5 M H_2SO_4 + 5 ppm HF.

	E_{corr} (V) (vs. SME)	I_{corr} (μA cm^{-2})	Relative I_{corr}
Plasma nitrided titanium	−0.858	−89.797	12.705
Pure titanium	−0.725	−7.113	1.006
Graphite	−0.493	−7.068	1

3.3. Potentiodynamic polarization

Fig. 6 shows the potentiodynamic polarization curves for pure titanium, plasma nitrided titanium and graphite in 0.5 M H_2SO_4 + 5 ppm HF. It is observed that the current density is decreased when increasing the potential. Then when the free corrosive potential was researched, the specimen surface changed from cathode polarization to anode polarization.

With a further increase in potential, the current density began to increase, that indicated a new corrosion. In comparison with the corrosion current densities of plasma nitrided titanium shown in Table 3, pure titanium and graphite exhibited much lower corrosion current densities. The results revealed that titanium nitride layer formed on the substrate had a poor corrosion resistance. That maybe because the titanium nitride layer was not dense and some corrosions that could be seen in Fig. 3(c) took place in the corrosive solution [21–23]. The good results on the pure titanium may be caused by the passive films produced in the corrosive system.

4. Conclusions

Different test samples were investigated via the interfacial contact resistance and potentiodynamic polarization tests. After plasma nitriding, the XRD results show an obvious titanium nitride and other transient phases formed on the titanium substrate. The plasma nitided titanium exhibits a much lower contact resistance compared with the pure titanium. However, the potentiodynamic electrochemical property is not improved because the titanium nitride coating has poor corrosion resistance. Some more improvements are expected in the plasma nitriding process or another surface modification on pure titanium.

Acknowledgement

This work is supported by the National High Technology Research and Development Program of China (863 Program) (Grant 2008AA03Z206).

References

[1] V. Mehta, J.S. Cooper, J. Power Sources 114 (2003) 32–53.
[2] V.M. Vishnyakov, Vacuum 80 (2006) 1053–1065.
[3] S.M. Haile, Acta Mater. 51 (2003) 5981–6000.
[4] T. Matsuura, M. Kato, M. Hori, J. Power Sources 161 (2006) 74–78.
[5] H. Tawfik, Y. Hung, D. Mahajan, J. Power Sources 163 (2007) 755–767.
[6] P.L. Hentall, J.B. Lakeman, G.O. Mepsted, J. Power Sources 80 (1999) 235–241.
[7] D.P. Davis, P.L. Adcock, M. Turpin, S.J. Rowen, J. Appl. Electrochem. 30 (2000) 101–105.
[8] A. Hermanna, T. Chaudhuri, P. Spagnol, Int. J. Hydrogen Energy 30 (2005) 1297–1302.
[9] J. Wind, R. Spah, W. Kaiser, G. Bohm, J. Power Sources 105 (2002) 256–260.
[10] F.M. El-Hossary, N.Z. Negm, S.M. Khalil, M. Raaif, Thin Solid Films 497 (2006) 192–202.
[11] L. He, X. Zhang, C. Tong, Surf. Coat. Technol. 200 (2006) 3016–3020.
[12] R. Hubler, Surf. Coat. Technol. 116–119 (1999) 1116–1122.
[13] F. Yildiz, A.F. Yetim, A. Alsaran, A. Celik, Surf. Technol. 202 (2008) 2471–2476.
[14] R. Tian, J. Sun, L. Wang, Int. J. Hydrogen Energy 31 (2006) 1874–1878.
[15] F. Gallianoa, E. Galvanettoa, S. Mischler, D. Landolt, Surf. Coat. Technol. 145 (2001) 121–131.
[16] Z. Xu, X. Liu, P. Zhang, Y. Zhang, G. Zhang, Z. He, Surf. Coat. Technol. 201 (2007) 4822–4825.

[17] J. Ihonen, F. Jaouen, G. Lindbergh, G. Sundholm, Electrochim. Acta 46 (2001) 2899–2911.
[18] L. Zhang, Y. Liu, H. Songa, J. Power Sources 162 (2006) 1165–1171.
[19] H. Wang, M.A. Sweikart, J.A. Turner, J. Power Sources 115 (2003) 243–251.
[20] S. Rudenja, C. Leygraf, J. Pan, P. Kulu, E. Talimets, V. Mikli, Surf. Coat. Technol. 114 (1999) 129–136.
[21] M. Li, S. Luo, C. Zeng, J. Shen, H. Lin, C. Cao, Corros. Sci. 46 (2004) 1369–1380.
[22] E. Galvanetto, F.P. Galliano, A. Fossati, F. Borgioli, Corros. Sci. 44 (2002) 1593–1606.
[23] Y. Wang, D.O. Northwood, J. Power Sources 165 (2007) 293–298.